MICROBOONE-NOTE-1126-PUB
FERMILAB-FN-1252-PPD

PROGRESS TOWARDS AN EXPANDED SEARCH FOR NEUTRAL-CURRENT DELTA RADIATIVE DECAYS IN MICROBOONE

June 11, 2024

The MicroBooNE Collaboration

microboone_info@fnal.gov

Abstract

In this note, we present progress toward an expanded search for neutral current Delta radiative decays (NC $\Delta \rightarrow N\gamma$) in MicroBooNE. We present sensitivities for several tests of the MiniBooNE Low Energy Excess (LEE) under NC $\Delta \rightarrow N\gamma$ scaling hypotheses, with significantly enhanced sensitivity relative to previous tests. These selections can also be used for additional single photon searches in the future, including searches which target more specific hadronic final states and particular regions of shower kinematic phase space.

This document was prepared by MicroBooNE Collaboration using the resources of the Fermi National Accelerator Laboratory (Fermilab), a U.S. Department of Energy, Office of Science, Office of High Energy Physics HEP User Facility. Fermilab is managed by Fermi Research Alliance, LLC (FRA), acting under Contract No. DE-AC02-07CH11359.

1 INTRODUCTION

MicroBooNE [1] is a Liquid Argon Time Projection Chamber (LArTPC) in the Booster Neutrino Beam (BNB) at Fermilab. One of MicroBooNE's primary goals is to investigate the MiniBooNE Low Energy Excess (LEE) [2]. Using the LArTPC technology, we can use the energy deposited per unit length at the trunk of the shower as well as gaps between showers and tracks in order to identify the single photon topology, and in particular NC $\Delta \rightarrow N\gamma$ events. We previously searched for this process in Ref. [3], and now we expand the search with additional selections which particularly enhance our sensitivity in the one photon zero proton ($1\gamma 0p$) channel. This note expands on the progress reported in Ref. [4].

We use the same selections as in Ref. [3], which use Pandora reconstruction [5], as well as new selections using Wire-Cell reconstruction [6, 7]. The Wire-Cell selection uses a Boosted Decision Tree (BDT) trained in a similar way as described in Ref. [8]. We apply a fully-contained cut, removing events with reconstructed charge near the TPC boundaries, as well as a BDT cut. We then split the events into two samples: zero reconstructed protons ($0p$), and one or more reconstructed protons (Np). For this purpose, we require that the protons have reconstructed kinetic energy greater than 35 MeV, corresponding to an expected track length equal to the gap between adjacent wires (3 mm). Reconstructed charged pions exist in a small fraction of the final selection.

To obtain systematic uncertainties, we follow the same procedure as was used in Ref. [8]. This procedure includes flux, cross section, hadron re-interaction, detector, and statistical uncertainties. There is a relatively small amount of events which appear in multiple channels, leading to statistical correlations, and these have been included in our covariance matrix. Additional uncertainties related to higher mass resonances, photonuclear absorption, and coherent single photon production have been considered and determined to be negligible. We constrain uncertainties using four sideband channels: NC π^0 Np, NC π^0 $0p$, ν_μ CC Np, and ν_μ CC $0p$.

In this note, we describe efficiencies and sensitivities to different LEE models.

2 EFFICIENCIES

Table 1 shows a summary of the efficiency and purity of each selection. Efficiency is calculated with respect to all simulated true NC $\Delta \rightarrow N\gamma$ events in the fiducial volume. In particular, note the improvement in the $1\gamma 0p$ channel using Wire-Cell relative to the existing Pandora channels.

	Wire-Cell $1\gamma Np$	Pandora $1\gamma 1p$	Wire-Cell $1\gamma 0p$	Pandora $1\gamma 0p$
NC $\Delta \to N\gamma$ eff.	4.09%	4.31%	8.78%	5.58%
NC $\Delta \to N\gamma$ pur.	9.95%	15.1%	8.79%	4.35%

Table 1: Efficiency and purity summary and comparison with the previous Pandora single photon analysis [3].

It is also worth noting that the selections are almost orthogonal. There are only 21 predicted overlapping events between the 176 Wire-Cell predicted events and the 191 Pandora predicted events. This small rate of overlap is somewhat surprising given that both analyses are targeting the same types of events; this indicates that there is significant room for future improvements in single photon reconstruction and selection.

3 HISTOGRAMS

Fig. 1a shows the constraining channels used in this analysis. Fig. 1b shows the signal channels, with data shown for the Pandora selections but with data still blinded in the Wire-Cell selections. The Pandora signal channel data is the same as in Ref. [3]. Fig. 2 shows the same information as Fig. 1b across two plots in a larger format.

4 LEE SENSITIVITIES

MiniBooNE reported that a 3.18 times enhancement of NC $\Delta \to N\gamma$ events would match the rate and radial distribution of the MiniBooNE excess events [2]. In this section, we consider three possible tests of that hypothesis.

First, we consider a two-hypothesis test. We calculate the difference in χ^2 values between the LEE and nominal hypotheses. The χ^2 values are calculated using signal and constraining channels and all correlations. We generate 30,000 toy experiments from our full covariance matrix including all systematic and statistical uncertainties, and use the median to evaluate sensitivities. The result is shown in Fig. 3. Note that the combined Wire-Cell+Pandora sensitivity to reject this LEE model is 2.13σ, a notable improvement over the prior sensitivity in Ref. [3].

Next, we consider a 1D scaling hypothesis. We consider the NC $\Delta \to N\gamma$ rate relative to our nominal prediction (x_Δ) as a free parameter, and create confidence intervals for this parameter. This can also be interpreted as confidence intervals in the effective $\Delta \to N\gamma$

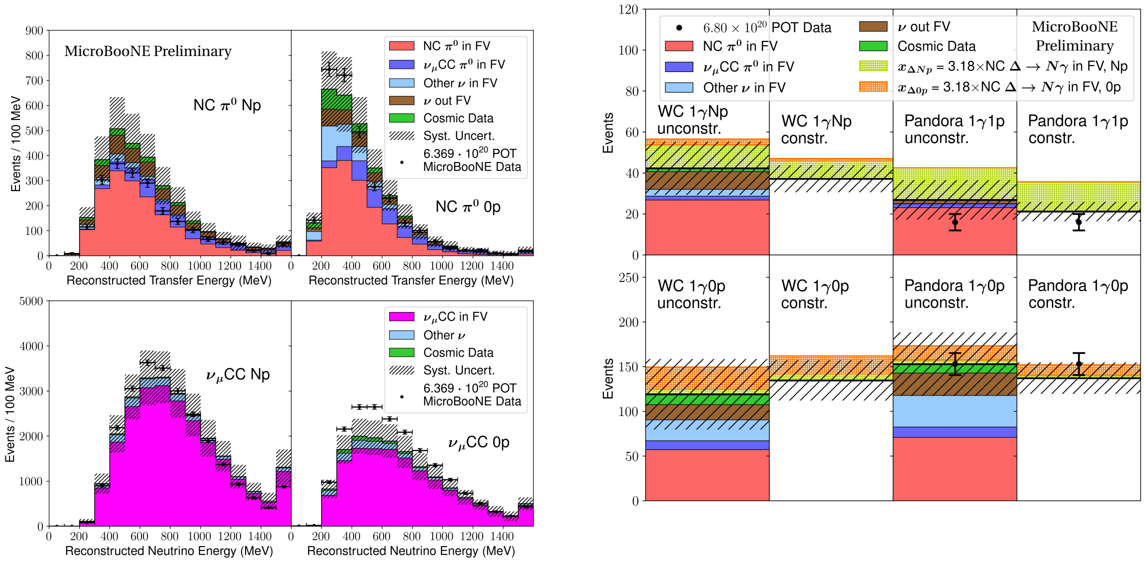

(a) (b)

Figure 1: (a): NC π^0 and ν_μCC constraining channels, with the rightmost bin in each subplot is an overflow bin. This uses 6.369×10^{20} POT of data processed through Wire-Cell reconstruction. (b): Signal channels, with the LEE prediction shown on top of the no-NC $\Delta \to N\gamma$ prediction. This uses 6.80×10^{20} POT of data processed through Pandora reconstruction. The Wire-Cell signal channel data is currently blinded.

branching fraction or the flux-averaged NC $\Delta \to N\gamma$ cross section. We consider a MiniBooNE error band on this parameter including statistical and systematic uncertainties, estimated using the 4.8σ significance of the LEE [2]. We use an Asimov data set with the measurement exactly equal to the prediction in order to evaluate the sensitivity. For each scaling point, we generate toy experiments, and calculate the confidence level as the percentage of toy experiments with a smaller $\Delta\chi^2 = \chi^2 - \chi^2_{\text{min}}$ than the data. The result is shown in Fig. 4a. In particular, we can see that the Wire-Cell + Pandora sensitivity improves on the Pandora-only result, with smaller expected error bars.

Note that our rejection of the NC $\Delta \to N\gamma$ scaling LEE hypothesis in our first NC $\Delta \to N\gamma$ analysis [3] primarily comes from the $1\gamma1p$ channel, which has significantly higher efficiency and purity compared to the $1\gamma0p$ channel, due to its more distinct topology which includes activity at the neutrino vertex. So if there is any MiniBooNE-like excess of events with an NC $\Delta \to N\gamma$ topology, it is likely to lie in the zero-proton channel. To account for this type of scenario, where an excess could lie more in one channel than another, we consider a 2D scaling hypothesis. Here, we split the NC $\Delta \to N\gamma$ signal into two components: those

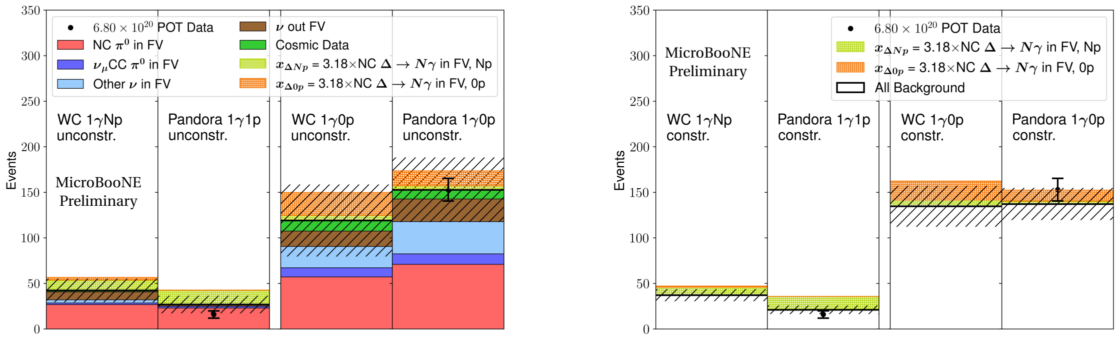

(a) (b)

Figure 2: (a): Unconstrained signal channels. (b): Constrained signal channels. Both show the LEE prediction shown on top of the no-NC $\Delta \to N\gamma$ prediction. This uses 6.80×10^{20} POT of data processed through Pandora reconstruction. The Wire-Cell signal channel data is currently blinded.

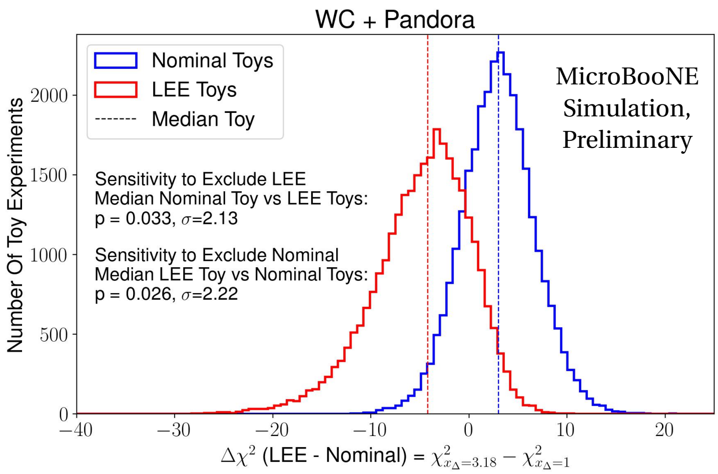

Figure 3: Wire-Cell + Pandora Two-Hypothesis test sensitivitity.

containing a true primary proton with greater than or equal to 35 MeV of true kinetic energy (Np), and those without any such true proton ($0p$). We consider scalings of each of these components, $x_{\Delta Np}$ and $x_{\Delta 0p}$. The MiniBooNE LEE can be interpreted as a total scaling of the rate of NC $\Delta \to N\gamma$ events, and therefore as a weighted sum of $x_{\Delta 0p}$ and $x_{\Delta Np}$ (NC $\Delta \to N\gamma$ events are 52.8% true Np and 47.2% true $0p$ in MicroBooNE with a 35 MeV true kinetic energy threshold). We use an Asimov data set to evaluate the sensitivity, and use Wilks' theorem to calculate confidence levels from the $\Delta\chi^2$ map. The result is shown in Fig. 4b. In particular, we see that the Wire-Cell + Pandora sensitivity improves on the Pandora-only sensitivity when considering large scalings of 0p events.

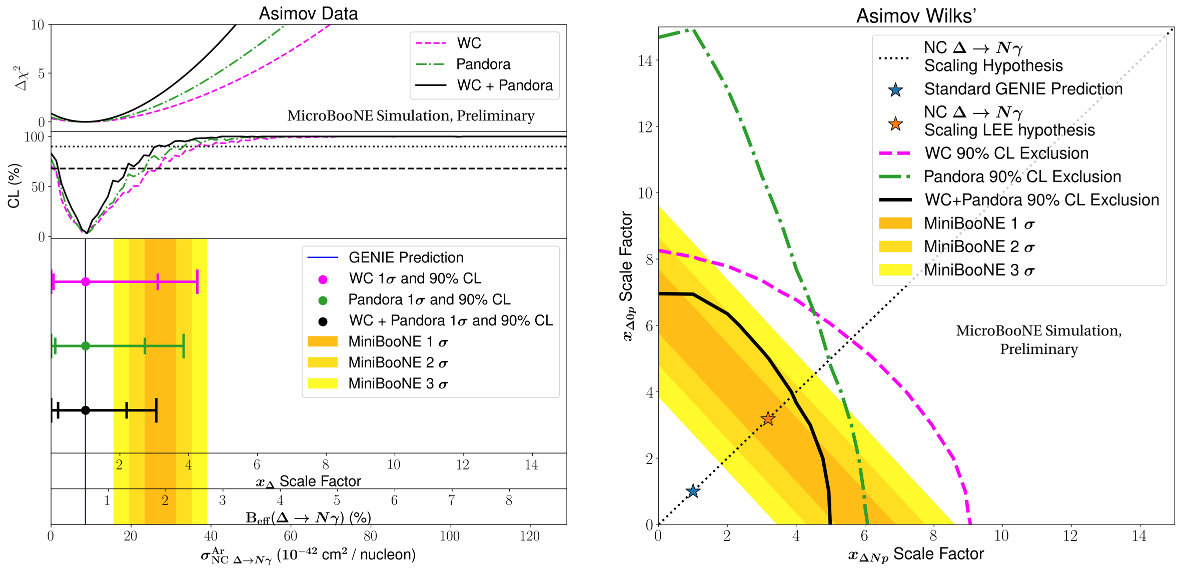

(a) (b)

Figure 4: (a): Sensitivity for the 1D NC $\Delta \to N\gamma$ scaling hypothesis. (b): Sensitivity for the 2D NC $\Delta \to N\gamma$ scaling hypothesis. The parameter space to the upper right of each curve is expected to be excluded at 90% CL.

5 CONCLUSIONS

This note introduces new NC $\Delta \to N\gamma$ selections using Wire-Cell reconstruction. This allows higher efficiency and higher purity for single photon events with no associated protons, as well as a large set of statistically independent data events. We demonstrate substantial increases in sensitivity for NC $\Delta \to N\gamma$ scaling LEE hypotheses. Additional single photon searches with different hadronic and shower kinematic distributions could be considered in the future using these selections.

References

[1] MicroBooNE Collaboration. Design and Construction of the MicroBooNE Detector. *JINST*, 12(02):P02017, 2017.

[2] MiniBooNE Collaboration. Updated MiniBooNE neutrino oscillation results with increased data and new background studies. *Phys. Rev. D*, 103:052002, Mar 2021.

[3] P. Abratenko et al. Search for Neutrino-Induced Neutral-Current Δ Radiative Decay in MicroBooNE and a First Test of the MiniBooNE Low Energy Excess under a Single-Photon Hypothesis. *Phys. Rev. Lett.*, 128:111801, Mar 2022.

[4] Progress Towards an Investigation of the MiniBooNE Low Energy Excess Using Neutral-Current Delta-Like Single Photons in MicroBooNE with Wire-Cell 3D Reconstruction Algorithms, MicroBooNE Public Note 1104, `http://microboone.fnal.gov/wp-content/uploads/MICROBOONE-NOTE-1104-PUB.pdf`.

[5] R. Acciarri et al. The Pandora multi-algorithm approach to automated pattern recognition of cosmic-ray muon and neutrino events in the MicroBooNE detector. *Eur. Phys. J.*, C78(1):82, 2018.

[6] MicroBooNE Collaboration. Neutrino event selection in the MicroBooNE liquid argon time projection chamber using wire-cell 3d imaging, clustering, and charge-light matching. *Journal of Instrumentation*, 16(06):P06043, Jun 2021.

[7] X. Qian, C. Zhang, B. Viren, and M. Diwan. Three-dimensional imaging for large LArTPCs. *Journal of Instrumentation*, 13(05):P05032–P05032, may 2018.

[8] Search for an anomalous excess of inclusive charged-current ν_e interactions in the MicroBooNE experiment using Wire-Cell reconstruction. *Phys. Rev. D*, 105:112005, Jun 2022.